

CS(AR)-20/96-97

DAM BREAK STUDY OF BARNA DAM



अने हि वा पशेयुः

NATIONAL INSTITUTE OF HYDROLOGY
JAL VIGYAN BHAWAN
ROORKEE - 247 667

CONTENTS

	Page No.
List of Figures	(i)
List of Tables	(ii)
ABSTRACT	(iii)
INTRODUCTION	1
NWS DAMBRK MODEL	3
Major Features of DAMBRK Model	3
DATA REQUIREMENT	6
Roughness Representation	8
Expansion/contraction coefficients	8
BARNA PROJECT	9
Data for Dam Break Study	9
DAM BREAK ANALYSIS	16
Dam Break Flood	16
Sensitivity of Various DAMBRK Inputs to Maximum Discharge and Elevation	19
SUMMARY	39
REFERENCES	41

LIST OF FIGURES

No.	Title	Page No.
1.	Front view of dam showing formation of breach.	7
2.	Off-channel storage (plan view)	7
3.	Command area of Barna dam.	10
4.	Elevation Vs. capacity curve	12
5.	Design flood hydrograph.	13
6.	Profiles of river bed, maximum discharge, and maximum elevation.	17
7.	Routing of dam break flood hydrograph.	18
8a.	Sensitivity of Manning's roughness n to maximum elevation.	25
8b.	Sensitivity of expansion coefficient (Exp) to maximum elevation.	26
8c.	Sensitivity of time of failure (t_f) to maximum elevation.	27
8d.	Sensitivity of breach width (B_W) to maximum elevation.	28
8e.	Sensitivity of breach elevation (B_{El}) to maximum elevation.	29
8f.	Sensitivity of side slope (z) to maximum elevation.	30
8g.	Sensitivity of inflow to maximum elevation.	31
9a.	Sensitivity of Manning's roughness n to maximum discharge.	32
9b.	Sensitivity of expansion coefficient (Exp) to maximum discharge.	33
9c.	Sensitivity of time of failure (t_f) to maximum discharge.	34
9d.	Sensitivity of breach width (B_W) to maximum discharge.	35
9e.	Sensitivity of breach elevation (B_{El}) to maximum discharge.	36
9f.	Sensitivity of side slope (z) to maximum discharge.	37
9g.	Sensitivity of inflow to maximum discharge.	38

LIST OF TABLES

ICB/10/19

No.	Title	Page No.
1.	Optional capabilities of NWS DAMBRK model.	5
2.	Salient features of Barna project.	14

ABSTRACT

The dam break analysis forms an integral part of the overall dam safety program of a country, and India too is not an exception to it. The hazards created by the flood resulting from a sudden, rapid, and uncontrolled release of water through a breach that forms in a dam need to be assessed to provide adequate safety measures in the event of such a catastrophic failure. The level of detail of hydrologic and hydraulic analyses needed to evaluate the consequences of a dam-breached flood depends on the danger to human life and the amount of property damage that would occur. If human fatalities are unlikely and if property damage potential is small, a simple procedure might provide an adequate description of the extent and timing of downstream flooding resulting from a dam failure. In this report a dam break study of Barna dam located in the State of Madhya Pradesh is carried out using the popular National Weather Service Dam Break Flood Forecasting (NWS DAMBRK) model to assess the likely maximum flood discharge and elevation to be attained in Bareli township (about 22 km downstream of dam) in the eventuality of dam failure. Besides computing the dam break flood hydrograph, a sensitivity analysis of various DAMBRK inputs is carried out and their effect on maximum discharge and elevation profiles is evaluated.

INTRODUCTION

Ever since the earliest dams were built, there have been dam failures. Approximately, 2000 failures of constructed dams throughout the world since the twelfth century and many thousands of more failures of natural dams have been recorded. During the last 100 years, there have been about 200 significant failures of constructed dams in which more than 11,000 people died, 6800 lives were lost in three failures alone: Vaiont, Italy, 1963 (2600); South Fork (Johnstown) Pennsylvania, 1889 (2200); and Machhu II Dam, Gujarat, India, 1974 (2000+) Thus, the hazards created by the flood resulting from a sudden, rapid, and uncontrolled release of water through a breach that forms in a dam need to be assessed for an Emergency Action Plan (EAP) in order to provide adequate safety to the inhabitants downstream in the event of such a catastrophic failure. The other preventive measures include flood plain zoning, flood plain mapping and issue of flood warnings. Therefore, pre-determination of warning time and area of inundation assuming a hypothetical dam break situation or utilizing the experience of historical data is a necessary exercise in dam safety analysis.

The existing dam break models range from simple computations based on historical dam failure data that can be performed manually to complex models that require computer analyses. The purpose of each model is to predict the characteristics (such as peak discharge or stage, volume and flood wave travel time) of a dam failure flood. The simplest estimation of the peak discharge and attenuation downstream from a failure involves empirical data from historic dam failures. Much of the available data on peak discharges from failures of constructed dams is summarized by Costa (1985).

Peak discharges, depths, and areas inundated downstream need to be known to minimize loss of life and property. Within the last decade, numerous computer programs have been developed to simulate dam-break hydrographs. Two popular examples are the HEC-1 program of the Corps of Engineers and the National Weather Service DAMBRK model (Fread, 1980). The National Weather Service DAMBRK model, modified by Land (1980b), uses a hydraulic routing procedure based on a

nonlinear implicit finite-difference algorithm for solving the equations of continuity and momentum. References to other programs can be found in Land (1980a, b). The purpose of these models is to predict the behavior of flood waters released from a dam failure. The initial outflow hydrograph from a failed dam is usually approximated by a triangle. After the dam break outflow hydrograph is determined by one of the methods described previously, it is routed through the downstream valley to compute peak discharge and elevation at the location of concern. These models usually require river cross-sections, Manning's n values, and upstream and downstream boundary conditions. Model output includes prediction of flood wave travel time, peak discharges and volumes at different locations downstream, and inundation areas.

Land (1980a) made some interesting comparisons among four dam-break flood-wave models by using data from three actual dam failures and provided suggestions for finding the most accurate, stable, and economical model to use. Dam failure models are constrained by inaccuracies in estimates of breaching characteristics such as timing, size, and shape; by estimations of roughness coefficients, volume losses, debris, and sediment effects; and by channel hydraulics inadequately described by one-dimensional flow equations. Consequently, results of dam break models can have large and significant errors, and operating the more complicated models can be a difficult task (Land, 1980a). In simulation, the user specifies the timing and shape of the final breach. Breach parameters have little impact on flood characteristics far downstream from the dam (Petrascheck and Sydler, 1984). Morphological characteristics of breaches in historic constructed dams are described by Johnson and Illes (1976) and MacDonald and Langridge-Monopolis (1984).

The aim of the present report is to carry out a dam break analysis of Barna dam situated in Madhya Pradesh, compute the dam break flood hydrograph, study the dam break flood wave propagation characteristics in the downstream Barna River, and to evaluate the effects of various DAMBRK inputs on maximum discharge and water elevation profiles.

NWS DAMBRK MODEL

The theoretical formulation of DAMBRK model comprises of two mechanisms: (i) Breach formation and (ii) Routing. The breach in a dam is characterized by its size, shape, and time of formation. In the case of earthen dams, the time of formation is much larger than that in the case of concrete dams. The DAMBRK model assumes that if the time of formation is larger than 10 minutes, the failure is treated as sudden and if it is greater than or equal to 10 minutes, the failure is assumed to be gradual. The sudden failure conforms with the failures of concrete dams and the gradual failure with the earthen dams. The breach may form due to overtopping implying that the water level in the reservoir has exceeded top of the dam and piping implying that the water level in the reservoir has been at a lower level than the top of the dam at the time of failure. The failure of earthen dams which exceedingly outnumber all other types of dams is taken up for illustration. The modeling approach assumes a finite size of breach in a dam structure and it gradually increases as time progresses until it is fully developed. The computing time interval being of the order of 10 minutes, the size is linearly varied with time.

The above described breach acts as a weir and the flow over this weir depends on the depth of flow measured from the breach crest at a time. The three different processes which affect the flow computation makes dam break modeling more complex. These processes include routing of the time varying inflow through the reservoir, breach formation with time, and routing of the flow through the downstream channel. The first component is for computing the water level in the reservoir at the dam site (upstream face) to ascertain the depth of flow above the crest of the breach, the second component is for determining the size of the breach with progressing time, and the third component is for determining depth and quantity of flow at the dam site, for ascertaining the effective depth of flow over the weir, and at downstream locations of the river. These components are integrated through mathematical equations which

are solved using an iterative scheme and thus, the quantity of flow and the levels attained all along the downstream river are computed. The major features of the model are described in the foregoing section.

Major Features of DAMBRK Model

The DAMBRK model has several in-built features to cope with the specific structural and flow situations. The much advocated concept of multiple dams in series is a classical example of the structural complexity to dam break flow estimation and it can be handled by DAMBRK model. The flow through a bridge or several bridges is another example that makes the routing mechanism much more complex. The flow situations can be described by the type of flow, viz. sub-critical or super-critical or a combination of sub-critical and super-critical, in either way. The DAMBRK model has various options for dealing with the various structural and flow combinations. These options are briefly described in Table 1. The data requirement for the commonly employed Option 1 is given in the following chapter.

TABLE 1. OPTIONAL CAPABILITIES OF DAMBRK MODEL

Option No.	Description
1	Reservoir storage routing to compute outflow hydrograph from reservoir with sub-critical dynamic routing of outflow hydrograph through entire length of downstream valley.
2	Reservoir storage routing to compute outflow hydrograph from reservoir with super-critical dynamic routing of outflow hydrograph through entire length of downstream valley.
3	Reservoir storage routing of outflow hydrograph from reservoir with super-critical dynamic routing of outflow hydrograph through upstream portion of downstream valley and sub-critical dynamic routing through downstream portion of downstream valley.
4	Same as Option 1 except reservoir dynamic routing to compute outflow hydrograph from reservoir.
5	Same as Option 2 except reservoir dynamic routing to compute outflow hydrograph from reservoir.
6	Same as Option 3 except reservoir dynamic routing to compute outflow hydrograph from reservoir.
7	Sub-critical dynamic routing of input hydrograph through a channel-valley.
8	Super-critical dynamic routing of input hydrograph through a channel-valley.
9	Reservoir storage routing to compute outflow hydrograph from reservoir with sub-critical dynamic routing of outflow hydrograph through downstream channel-reservoir having a dam which may fail.
10	Reservoir dynamic routing to compute outflow hydrograph from reservoir with sub-critical dynamic routing of outflow hydrograph through downstream channel-reservoir having a dam which may fail.
11	Simultaneous computation method for single dam or bridge (structure) using dynamic routing in the reach upstream of the structure and downstream of the structure with special internal boundary conditions for flow through the structure.
12	Simultaneous computation method for multiple dams and or bridges (structures) using dynamic routing for all reaches with special internal boundary conditions for flow through each structure.

DATA REQUIREMENT

The input data requirement for the DAMBRK model can be categorized into two groups as follows.

The first data group pertains to the dam, the breach, spillways and physical characteristics of the reservoir. The breach data consist of the following parameters as also shown in Fig. 1:

- time of breach formation, (hr)
- final bottom breach width, b (ft)
- side slope of breach, z (ft/ft)
- final elevation of breach bottom, h_{bm} (ft)
- initial elevation of water level in the reservoir, h_o (ft)
- elevation of water when breach begins to form, h_f (ft)
- elevation of top of dam, h_d (ft)

The spillway data consist of the following:

- elevation of uncontrolled spillway crest, h_s (ft)
- coefficient of discharge of uncontrolled spillway, C_s
- elevation of centre of submerged gated spillway, h_g (ft)
- coefficient of discharge of gated spillway, C_g
- coefficient of discharge of crest of dam, C_d
- constant head independent discharge from dam, Q_t (cusec)

The Q_t is the discharge that takes place from the dam in the form of seepage. The reservoir data consist of a table describing the storage features of the reservoir, surface area (acre) or volume (acre-ft) versus elevation (ft).

The second group of data pertains to the cross-sectional features of the downstream river. The cross-sections are specified by location in mile from the dam site. These are described in the form of a table reflecting variation of top widths (ft) with elevation (ft). It is to note that the elevation can be measured with reference to any arbitrary datum or above mean sea level. The top widths consist of inactive and active widths. The active width of flow is determined by visual inspection. It is the width of flow that allows discharge to take place in the river. On the other hand, the inactive width does not allow water to flow across a section of the river. The water so stored is known as off-channel storage. The backwater water in a tributary is an example of off-channel storage. It can be described by three cross-sections (Fig. 2):

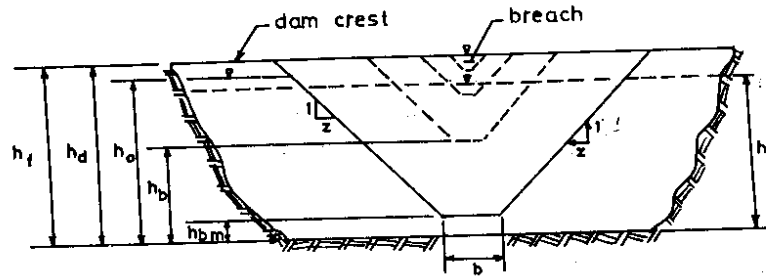


FIG. 1: FRONT VIEW OF DAM SHOWING FORMATION OF BREACH

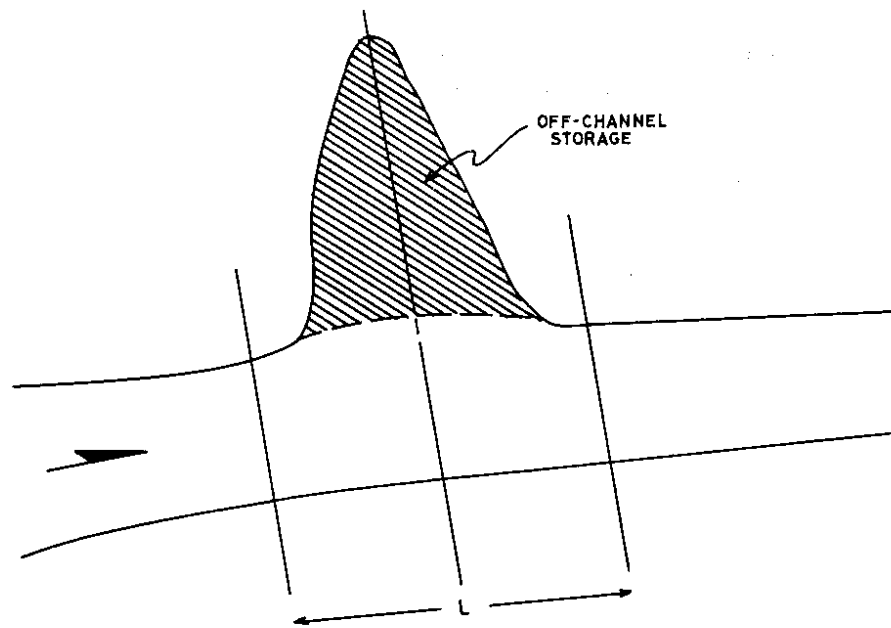


FIG. 2: OFF-CHANNEL STORAGE (PLAN VIEW)

One on the upstream end of the off-channel storage portion, one on the downstream end of the off-channel portion, and the other in the middle of it. The inactive width (BSS) for the middle cross-section is computed as below:

$$BSS = \frac{2.54}{L} \quad (1)$$

where BSS is the off-channel storage width (ft) for middle cross-section at an elevation (ft) and SA is the surface area of off-channel storage in square feet at that elevation (ft). Implicit in this treatment is the assumption that the time required by the water to occupy and evacuate this off-channel portion is negligible. This assumption will not hold if the tributary of concern is long for which filling and draining times are significant relative to the time required for a flood wave to pass the mouth of the tributary. A different treatment would be necessary to model it accurately.

The other properties of the river include hydraulic resistance and expansion-contraction coefficients.

Roughness Representation

Boundary resistance is reflected in the equation of motion through the friction slope, viz. Manning's equation. Friction slope is determined for a reach in terms of an arithmetic average of hydraulic radii for the effective flow portions of cross-sections at each end of the reach. The Manning's roughness coefficients (n-values) for varying elevations of flow are supplied to the DAMBRK model as input.

Expansion-contraction Coefficients

The expansion-contraction coefficients are determined from the geometry of the river. The contraction coefficient varies from 0.1 to 0.3 and the expansion coefficient varies from -0.5 to -1.0. These assume a zero value if the contraction and/or expansion between two consecutive cross-sections is negligible.

BARNA PROJECT

Barna project is an irrigation scheme across River Barna, a tributary of River Narmada. It is located near village Bari of Raisen district in Madhya Pradesh about 105 km from Bhopal and 70 km from Obey-Tallaganj railway station on the Jabalpur-Jaipur National Highway No. 12. The project construction was affected by the Indo-China war in 1962 and Indo-Pak war in 1965. Finally, the project was completed in 1978. On the right of the main dam, there is a saddle dam from which a 0.65m long joint water carrying canal emerges. From this canal two canals emerge from its left and right banks for irrigating the command area falling on its left and right banks, respectively.

The project came up with the objective to irrigate 42,956 ha land in Raisen district and 11,918 ha land in Sehore district. The irrigation from the dam started in 1975-76. The development works of irrigation drainage in the command (Fig. 3) started in 1981-82 by the Department of Water Resources. Initially, irrigation started from 5555 ha and had gone on increasing regularly. The irrigation drainage works have greatly improved the irrigation potential in the command and benefited the farmers of the command.

The project does not provide flood protection. However, through judicious and cautious reservoir operation, peaks can be moderated to some extent to subside the damage and submergence of life and properties in the downstream of the dam site, specially near Barley township.

Data for Dam Break study

In the downstream flood plains of the dam, there is a major city Bareilly at about 22 km from dam. As the present study aims at to study the likely flood scenario in and around this city in the dam break situation, the available two cross-sections, one at the dam site and the other at the Bareilly gauging site, were substantiated by the available contour map of the area. The major dam and reservoir features were derived from Table -1, providing salient features of the project. The elevation-area-capacity table

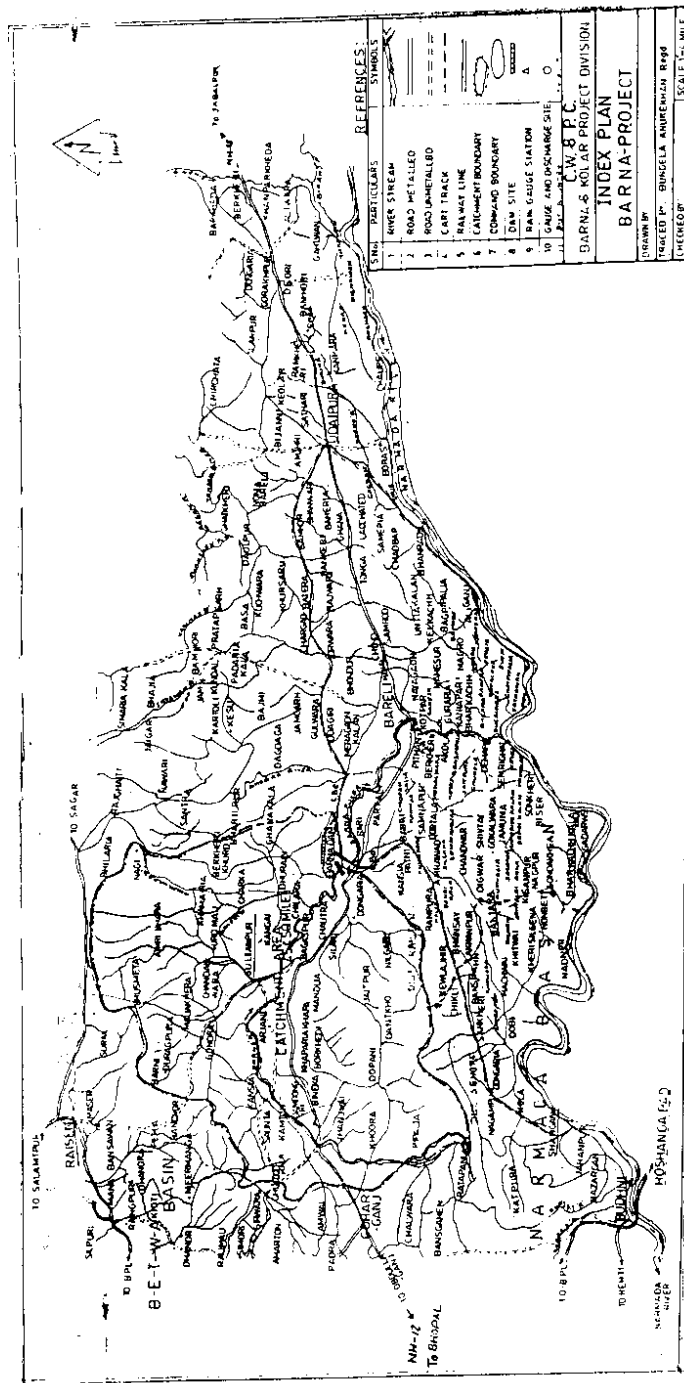


Fig. 3. Command area of Barua dam.

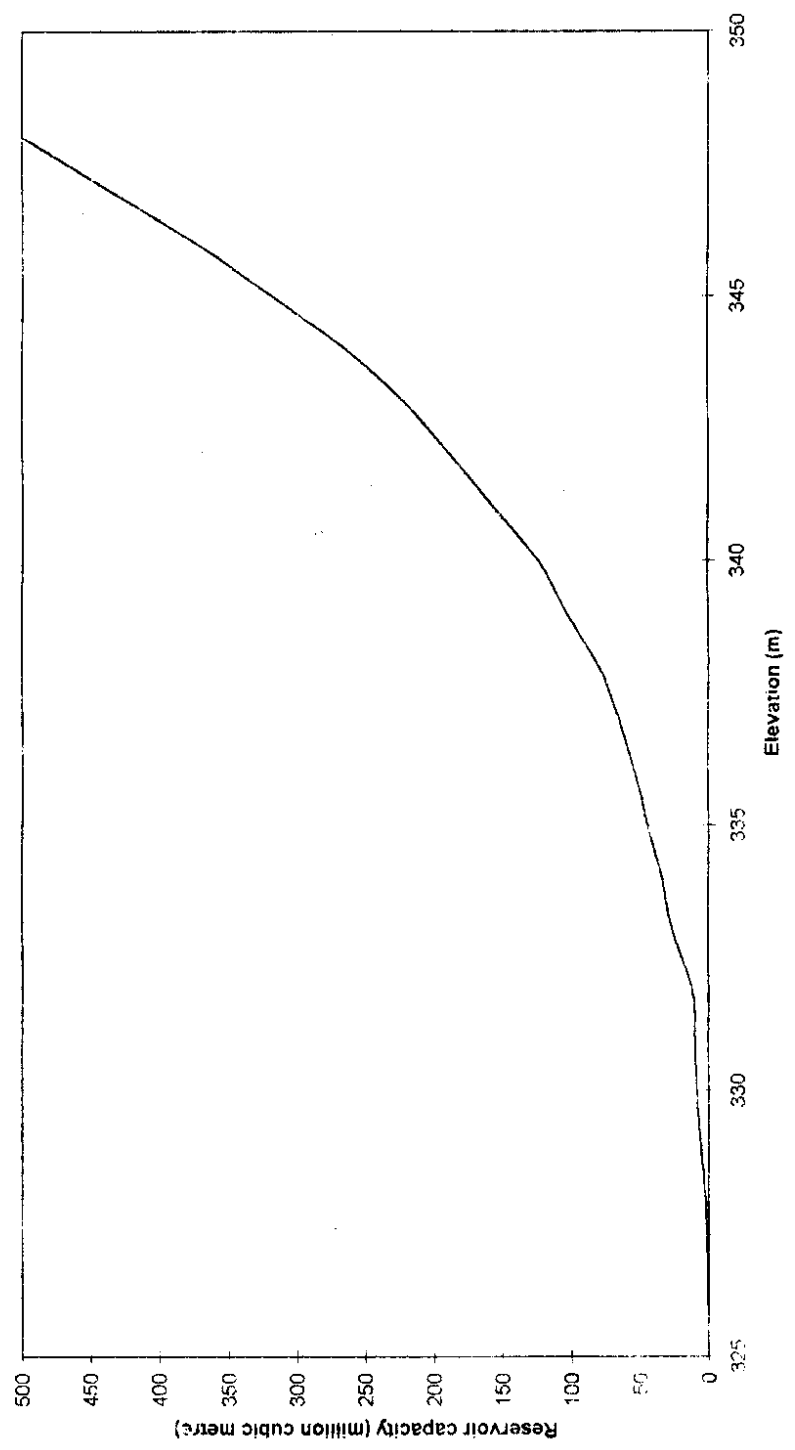
which was available from the dam site is used in the dam break analysis and is shown graphically in Fig. 4.

The designed maximum flood (PMF) is 13,557 cumec and the moderated flood at the maximum water level, 351.45 m, is 6825 cumec. The design flood hydrograph is given in Fig. 5. The discharge through radial gates is computed using the formula:

$$Q = M L (H_1^{3/2} - H_2^{3/2})$$

in FPS units. Here M is the coefficient that depends on gate opening, L is the length of radial gates in ft, H₁ is the depth of water above crest in ft, and H₂ is the depth of water above gate opening in ft. The project report of the dam provides complete computations for discharges at various gate openings.

Fig. 4. Elevation versus capacity curve.



FLOOD IN LAKHS CUSECS
L.C.M. = 26000 CUSECS

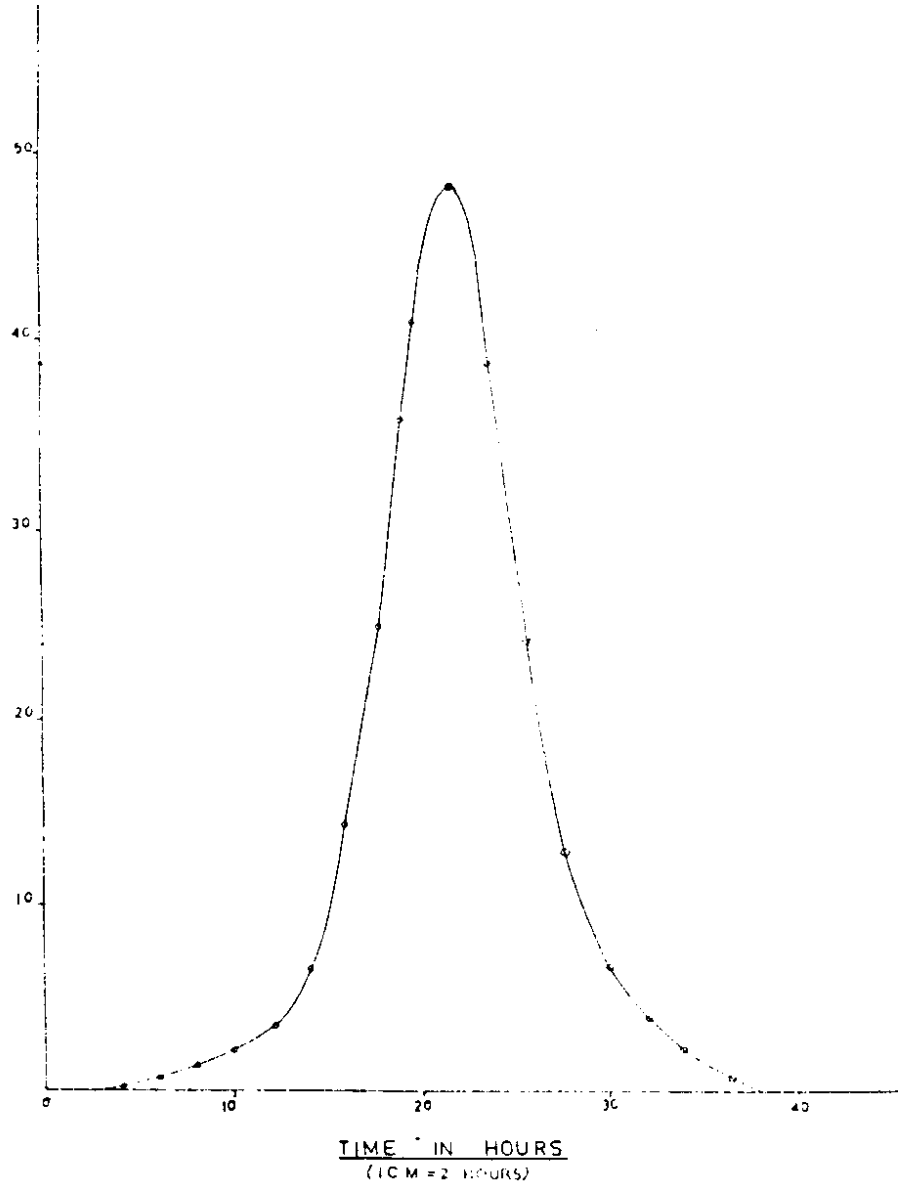


Fig 5. Design flood hydrograph.

TABLE 2. SALIENT FEATURES OF BARNA PROJECT

LOCATION

1. State	: Madhya Pradesh
2. District	: Raisen
3. Dam site location	: Longitude: 78°7', Latitude: 23°5'
4. Topo Sheet No.	: 55-1/4

HYDROLOGY

1. Drainage area of the river above dam site	: 1176 km ²
2. Average annual rainfall	: 1132 mm
3. Maximum annual rainfall	: 2068 mm (year 1973)
4. Minimum annual rainfall	: 535 mm (year 1920)
5. Mean annual runoff at the dam site	: 56,500 hect. m
6. Observed maximum flood discharge at the dam site	: 11,480 cumec (year 1965)
7. Design flood	: 13,557 cumec
8. Moderated flood	: 6825 cumec

RESERVOIR

1. Gross storage capacity at F.R.L. 348.55 m	: 53,900 hect.-m
2. Dead storage at L.S.L. 338.1 m	: 8,320 hect.-m
3. Live storage at F.R.L. 348.55 m	: 45,580 hect.-m
4. Area submerged at F.R.L. 348.55 m	: 7,700 hect.
5. i) Area under cultivation	: 2,430 hect.
ii) Area not under cultivation	: 2,190 hect.
iii) Forest area	: 3,080 hect.

6. No. of villages affected : 25

MAIN DAM

1. Type of dam : Straight gravity stone masonry
concrete dam

2. Normal pondage level : 348.55 m

3. Maximum water level : 351.45 m

4. Dead storage level : 338.1 m

5. Top level of dam : 352.70 m

6. Deepest reservoir bed level : 315.6 m

7. Length of dam : 4.60 m

8. Top width of dam : 4.60 m

9. Maximum height : 47.7 m

CENTRAL SPILLWAY

1. Crest level : 341.70 m

2. Length : 115.1 m

3. Type of gates : Radial gates

4. No. and size of gates : 8 nos., 12.2m x 6.85 m

5. Top level of crest gates : 348.55 m

SADDLE DAM

1. Type of dam : Straight gravity stone masonry
concrete

2. Length : 94.50 m

3. Top width : 4.6 m

4. Maximum height : 20 m.

DAM BREAK ANALYSIS

Dam Break Flood

Using the data described earlier, a dam break analysis of the Barna dam was carried out and the computed maximum discharge and maximum elevation profiles along with the river bed profile are shown in Fig. 6. Apparently, the maximum discharge values go on decreasing along the river downstream whereas the maximum elevation profile shows a linearly decreasing trend along the river, downstream of the dam, in the reaches where the river bed profile is uniformly lowering. For example, before approximately 17 km from the dam, the river bed is mild where the reduction in the maximum elevations at different locations in the reach is quite mild and at locations where the river is steep, these show a sharply decreasing trend. The greater the slope, the greater is the velocity and the lower will be the stage or elevation for a given discharge, as is apparent from the figure that the discharge is almost constant in the sub-reach after approximately 17 km.

The phenomenon of reducing discharges in a mild reach is attributed to wave propagation characteristic. The wave being more dynamic in a milder reach than in a steeper reach attenuates more than that in a steeper reach (Mishra and Seth, 1994, 1996; Mishra et al., 1997; Mishra and Singh, 1998a). Therefore, greater attenuation is visible in the sub-reach before 17 km from dam and almost no attenuation in the reach after 17 km, where the wave is kinematic due to the steep bed slope. The non-reduction of maximum elevations along the river downstream at the rate maximum discharges reduce along the river can be described by the channel tendency of first increasing velocities at a stage till it exhausts its carrying capacity and then the stage in an otherwise situation (Mishra and Singh, 1998b). In the river portion after 17 km from the dam site, maximum elevations go on reducing to maintain a consistency in the depth of flow with the river bed, which lowers with the increasing slope.

The above wave phenomenon can also be explained from Fig. 7, depicting the dam break flood hydrograph (at the dam site) along with the other hydrographs at various locations in the Barna river downstream of the dam. Up to 17 km representing

Figure 6 shows the profiles of river bed, maximum discharge, and maximum elevation. The x-axis represents the distance from the dam in kilometers (km), ranging from 0 to 35. The left y-axis represents Discharge in cumec, ranging from 0 to 90,000. The right y-axis represents Elevation in meters (m), ranging from 285 to 340. The legend indicates three data series: River bed elevation (represented by triangles), Maximum discharge (cumec) (represented by circles), and Maximum elevation (m) (represented by squares).

Fig. 6. Profiles of river bed, maximum discharge, and maximum elevation.

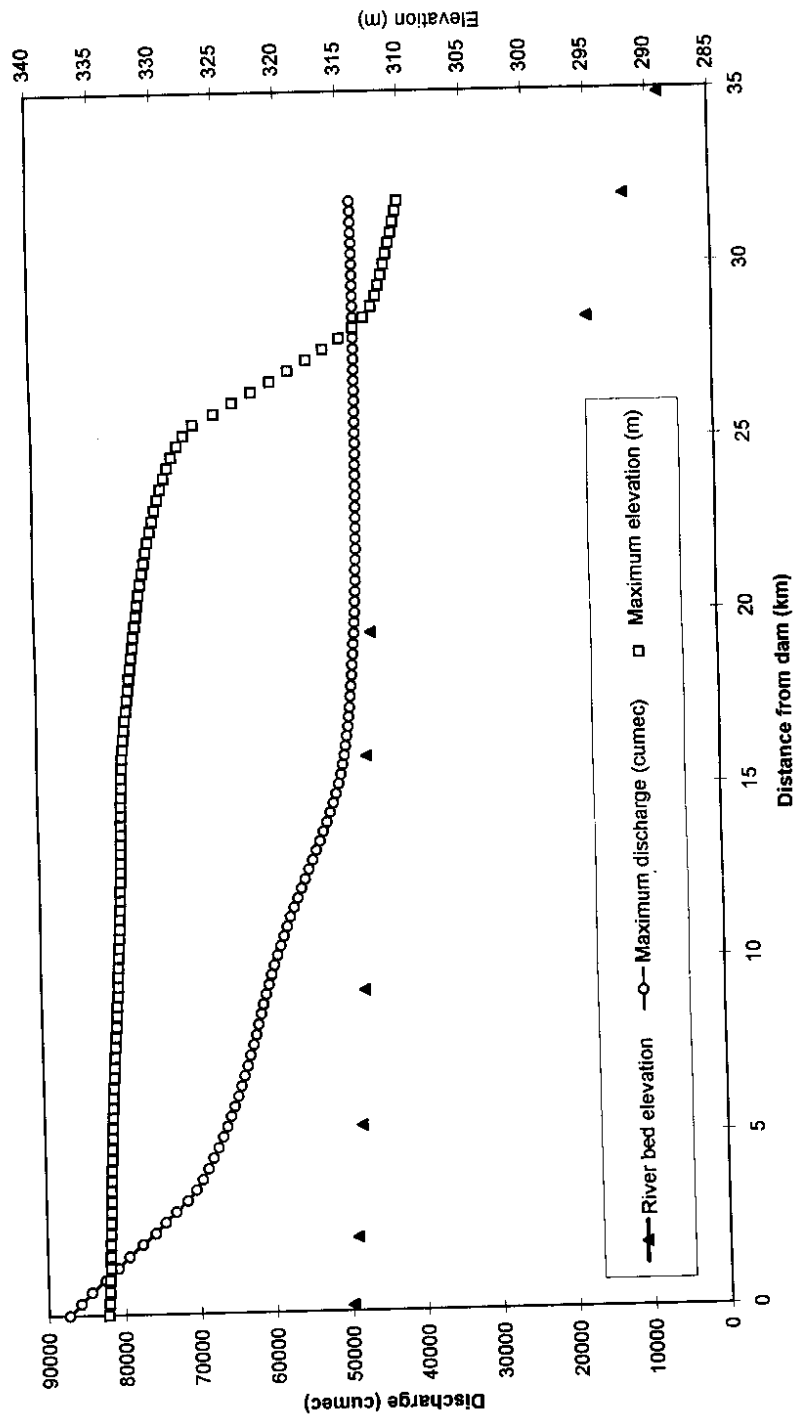
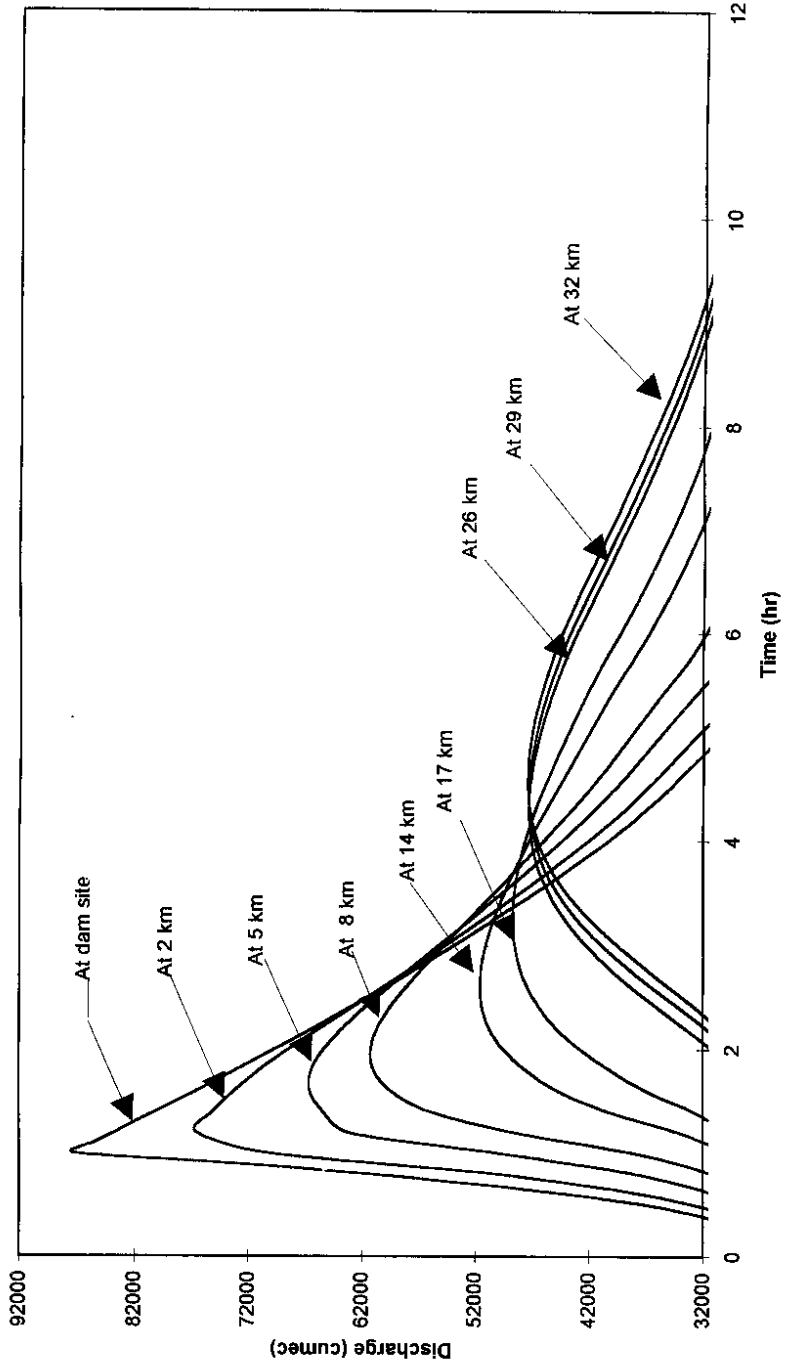


Fig. 7. Routing of dam break flood hydrograph.



a mild channel slope of the sub-reach and thus, a dynamic wave in this sub-reach, the flood hydrographs attenuate sharply whereas a little or no attenuation is apparent in the hydrographs at locations after 17 km. The wave only translates in the river portion after 17 km where the wave is a kinematic wave showing the significance of body forces being much larger than the inertial and/or pressure forces (Ferrick, 1985).

Sensitivity of Various DAMBRK Inputs to Maximum Discharge and Elevation Computations

To show the effect of various DAMBRK model inputs on maximum discharge and elevation computations a sensitivity analysis is carried out. The considered inputs are:

- a) Manning's roughness
- b) Expansion/contraction coefficients
- c) Time of failure
- d) Breach width
- e) Breach elevation
- f) Side slope of the breach section
- g) Inflow hydrograph.

These inputs are specifically considered because these data are supplied a priori for dam break flood computation and inhere a significant amount of uncertainty. These values are commonly subject to modeler's experience and judgment. It is, therefore, necessary to assess their impact on the dam break flood hydrograph and its propagation downstream in the uncertain environs, which, in turn, leads to carrying out a sensitivity analysis.

a) Effect of Manning's 'n'

In wave propagation, the Manning's roughness impedes the wave speed (or velocity) through the process of energy loss (Mishra and Seth, 1994, 1996; Mishra and Singh, 1998a). This lost energy is eventually dissipated in the atmosphere through

the bounding walls of the channel or the water surface. This, impediment affects (reduces) the discharge carrying capacity of the channel and thus leads to increasing the depth of flow for a given discharge at higher n -values. These trends are apparent in Figs. 8a showing maximum water elevation profile and 9a showing the profile of maximum discharge for Manning's roughness, varying from 0.035 to 0.045. At a higher n -value, the maximum discharge at a location reduces and the maximum elevation at that location increases. It is consistent with the law of conservation of energy (Mishra and Singh, 1998a). As the discharge or velocity (or kinetic energy) decreases, the depth of flow or pressure energy increases.

It is visible from Figs. 8a and 9a that the deviation in maximum elevation and discharge is more pronounced in respectively mild and steep river reaches. Interestingly, the dam break flood hydrograph (at the dam site or 0 km in Fig. 9a) remains almost unaffected of the roughness variation whereas maximum discharges at the other locations downstream show a consistently increasing deviation along the river. It implies that the effect of roughness is less pronounced at higher discharges than at lower discharges. As the dam break flood wave attenuates or peak discharge magnitudes go on decreasing as the wave propagates downstream, the downstream location of concern is more affected by the Manning's roughness than the dam break flood hydrograph at the dam site itself.

Also visible from Fig. 8a is that the more deviation is apparent in the mild river reach (before 17 km) and it almost diminishes in the steep river reach (after 17 km). It infers that the maximum elevation is more affected by the Manning's roughness at locations where the channel is mild than at locations where the river is steep.

b) Effect of expansion/contraction coefficients

The effect of expansion or contraction coefficients on maximum water elevation and discharge computations is analogous to that of Manning's roughness. As the magnitude of expansion or contraction coefficients increases, the more energy is lost (Mishra and Singh, 1998a) and thus, imposes greater impediment and, in turn, causes a reduction in discharge magnitude or increase in depth of flow (or elevation)

for a given discharge magnitude. The channel geometry, however, plays a significant role in balancing these actions. In the case of channel expansion, the river expands and thus, provides a larger right of way to the flood to pass at a particular depth of flow or for a given magnitude of discharge the depth of flow decreases. The converse is true for the case of channel contraction. How significantly the variation in the magnitude of expansion/contraction coefficients affects maximum discharge and elevation computation is investigated by varying only expansion coefficient. Here, expansion coefficient values are varied irrespective of river geometry, whether or not actually expanding.

Figs. 8b and 9b show the effect of expansion coefficients on maximum elevation and discharge profiles for the investigated range of coefficients varying from 0.0 to 1.0, the range stipulated by the DAMBRK manual (Fread, 1980). Evidently, as the expansion coefficient increases, the stages (or elevations) almost remain unaffected except in the most downstream part (after approximately 25 km from dam) and maximum discharges show a continually increasing discharges (from those due to lesser values of coefficients) at locations downstream, the greatest in the most downstream portion where the river bed is steep. A close investigation reveals that the increasing trend in discharge magnitudes is actually attributed to the expanding river geometry in the downstream portion.

c) Effect of time of failure

Time of failure is the time taken in the formation of breach to its full size as it is assumed that the dam being a earthen dam breaches gradually (Fig. 1). The larger the time of failure, more time the breach will take to develop fully and by that time more volume of runoff will pass through the breach into the downstream channel leading to reducing more the water elevation in the reservoir behind the dam. The lesser the water surface elevation in the reservoir, the lesser will be the depth of flow over the uncontrolled weir crest and the crest of the breach at the time breach is fully matured, leading to more reduction in the magnitude of peak discharge passing jointly through these weirs. The lesser magnitude of peak discharge will result in a lesser depth of peak flow downstream. This phenomenon is evident from the results of Figs. 8c and 9c,

depicting maximum water elevation and maximum discharge profiles, respectively, for the time of failure ranging from 0.5 hr to 1.5 hr. The phenomenon is more distinct in Fig. 9c. The time of failure of 1.5 hr reduces more the maximum discharge at a location in the downstream of river reach than any of the other magnitudes of time of failure and this trend continues in the whole river reach. The effect of time of failure on the maximum water elevation is much less pronounced than the maximum discharge. It implies that the effect of time of failure is to affect more maximum discharges than maximum elevations.

d) Effect of breach width

The breach width is the final length of the breach crest (Fig. 1). The effect of breach width is to affect the size of breach, which is responsible for providing an additional passage (besides uncontrolled weir) for flow to exit from reservoir (dam). The greater the size of breach width, the greater will be the size of breach at a time and will allow to pass a greater magnitude of discharge from the breached section. It leads to increasing the discharge magnitudes and thus, the maximum discharge. The greater discharges result in greater magnitudes of corresponding elevations at locations in the downstream river valley. Such a phenomenon is apparent from Figs. 8d and 9d, showing maximum elevation and maximum discharge, respectively, for breach widths ranging from 150 m to 300 m. The breach width of 300 m produces highest magnitudes of discharge and corresponding elevation at a location in the river reach and the breach width of 150 m produces lowest. In the case of maximum elevation (Fig. 8d), the effect almost diminishes in the steep river reach (after 17 km).

e) Effect of breach elevation

Breach elevation is the final elevation attained by the breach and corresponds to the final breach width (Fig. 1). Theoretically, the effect of the final breach elevation is again to provide a passage area for the flow from the reservoir or dam. The lower the elevation, the lesser will be the total area of cross section available to pass the discharge when the breach is fully developed. The converse is true in an otherwise situation. However, in the present case study, the effect of breach elevation on both

maximum water elevation and discharge is not much significant. It is attributed to the fact that the total area of cross-section required for the peak discharge to pass through, when the breach is fully developed, is sufficient in any of the considered cases and does not lend to increasing or decreasing discharge and, in turn, the elevation at the dam site and, therefore, at any other location in the downstream river reach.

f) Effect of Side Slope

The side slope is the lateral slope of trapezoid of the breach section as shown in Fig. 1. The effect of the side slope is again to affect the area of breach section at a time and, therefore, the dam break discharge and, in turn, elevations downstream. Its impact on maximum water elevation and discharge is shown in Figs. 8e and 9e, respectively, for the side slopes ranging from 0.015 to 0.045. The insignificant effect on both the maximum water elevation and discharge is attributed to the above-described fact that the area of cross-section required for the peak dam break discharge, when the breach is developed fully, is more than sufficient in any of the cases examined.

g) Effect of inflow magnitude

The inflow is the discharge coming into the reservoir at the time dam breaches. It actually contributes to building up of reservoir storage at a time and if the augmented storage is significant compared to the existing storage in the reservoir, it will substantiate to increasing the dam break discharge magnitude at that time. It is worth noting that in the present study, only recession limb of the hydrograph is considered keeping in view that the rising limb of the hydrograph has contributed to taking the reservoir to an elevation (the initial reservoir elevation in DAMBRK input data) leading the dam to breach or fail. Since the dams are continuously monitored for rising water elevation in reservoirs in a flood season, the above hypothesis is reasonably close to the actual process of dam failure.

The above phenomenon can be visualized from Figs. 8g and 9g showing maximum water elevation and discharge profiles, respectively, for the inflow magnitudes ranging from 50% of design flood to 150% of design flood. The greater

magnitudes of inflow cause greater magnitude of peak dam break discharge and, therefore, the peak elevation at the dam site and at other locations downstream. A close investigation reveals that the effect on discharge is more pronounced in the river portion having steep slope (after 17 km) and the converse is true in the case of elevation.

Fig. 8a. Sensitivity of Manning's roughness n to maximum elevation.

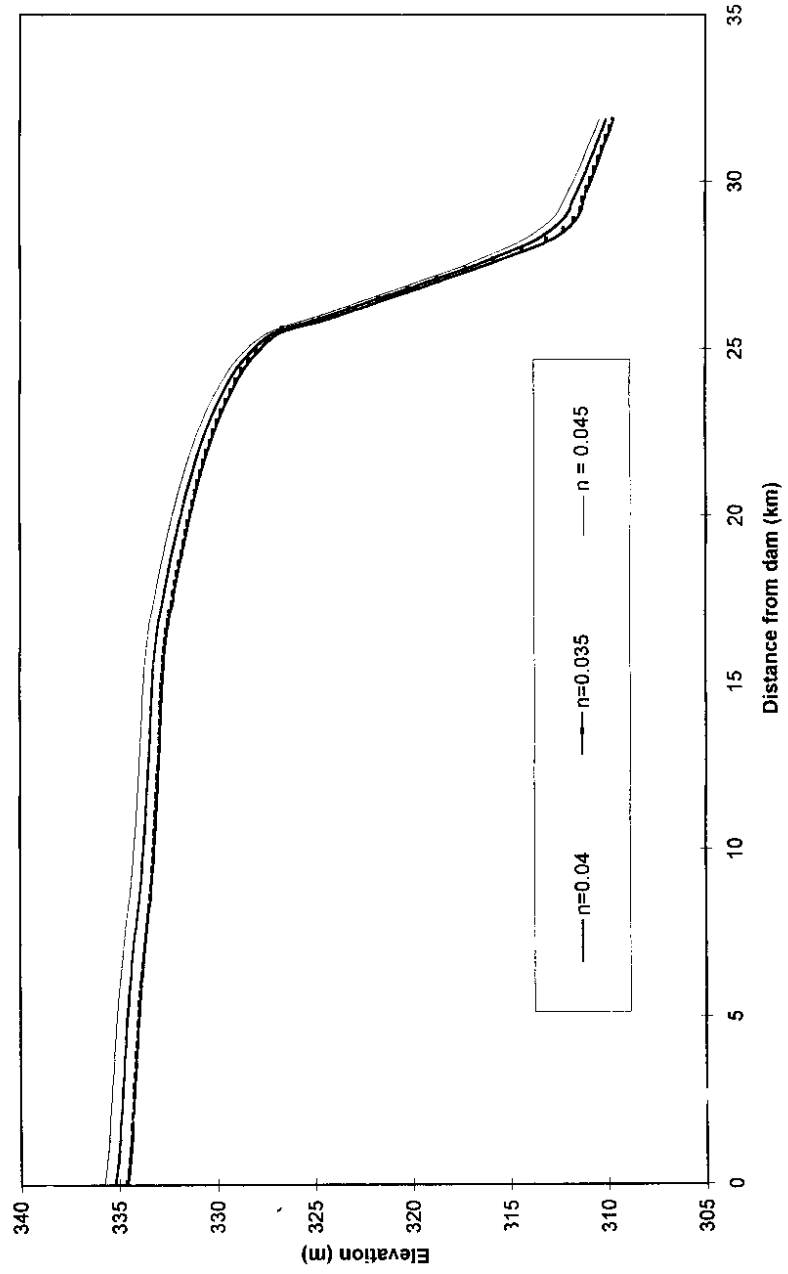


Fig. 8b. Sensitivity of expansion coefficient (Exp) to maximum elevation.

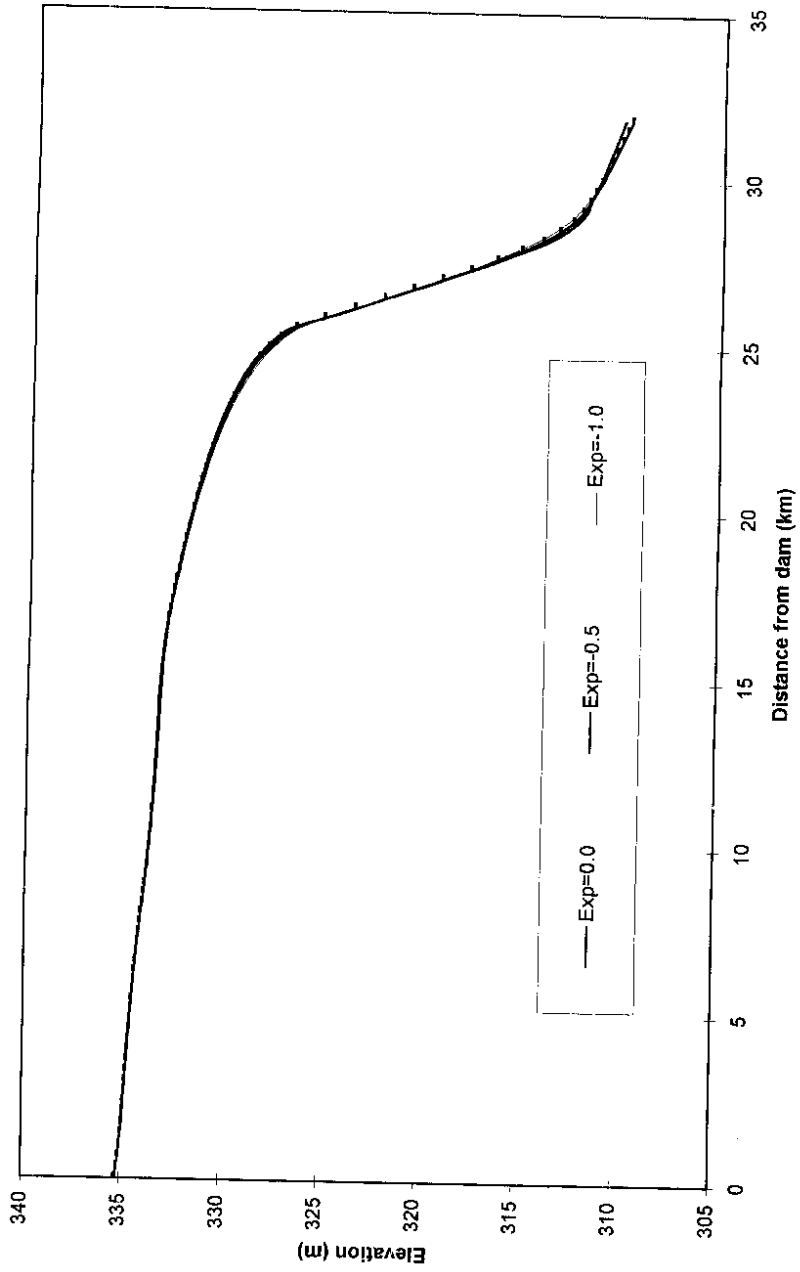


Fig. 8c. Sensitivity of time of failure (t_f) to maximum elevation.

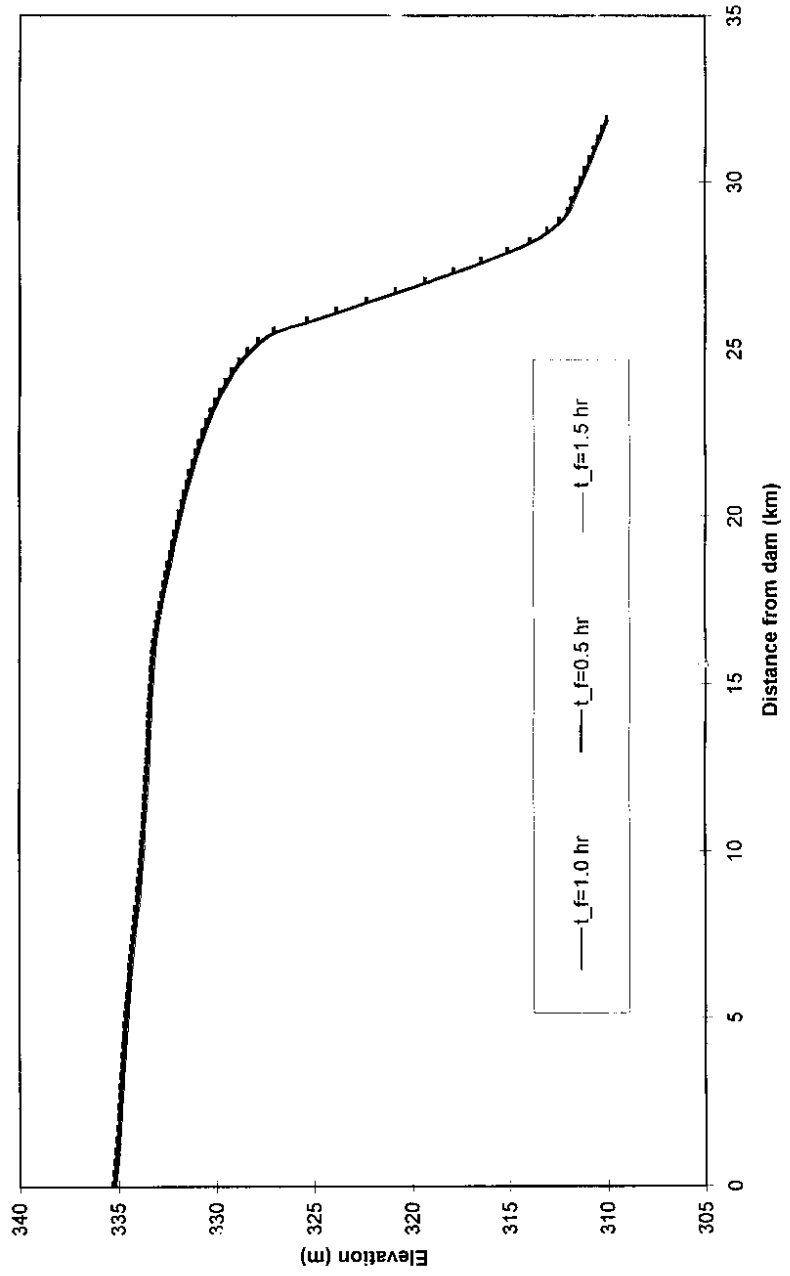


Fig. 8d. Sensitivity of breach width (B_W) to maximum elevation.

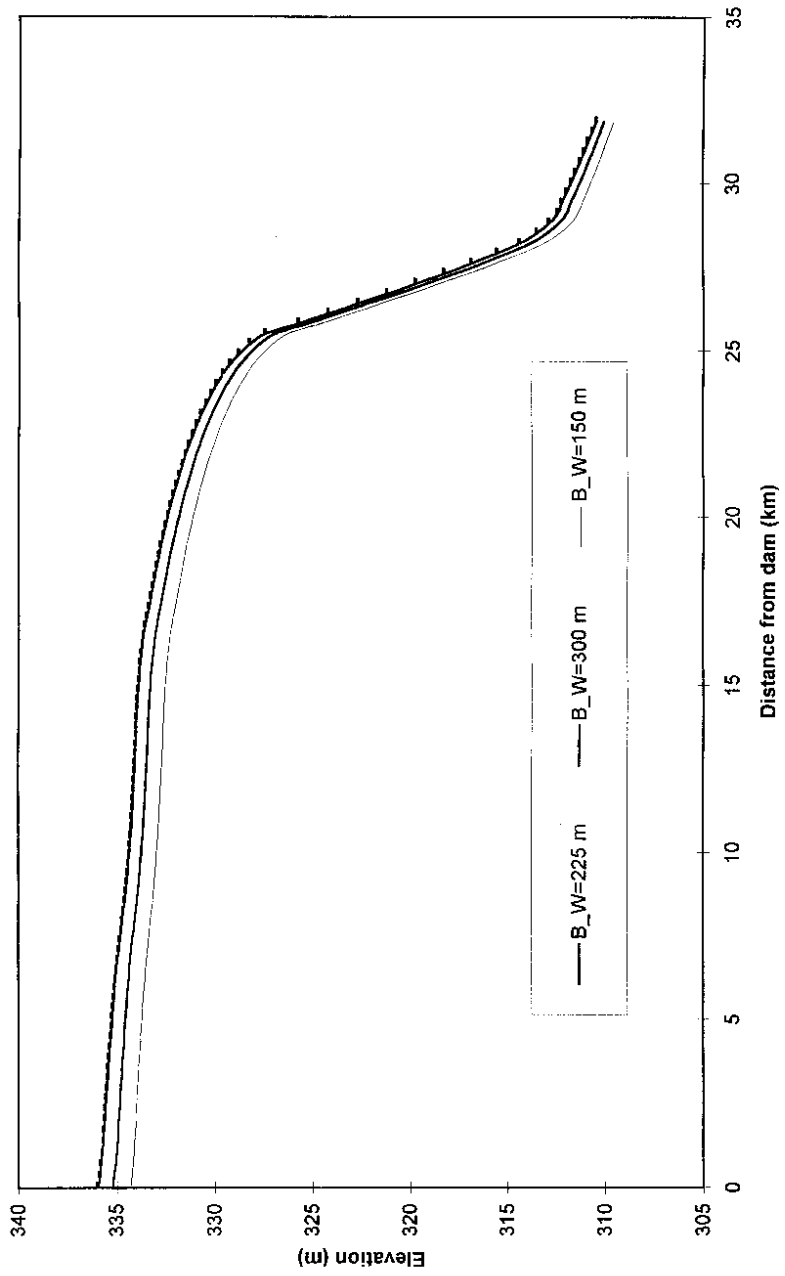


Fig. 8e. Sensitivity of breach elevation (B EI) to maximum elevation.

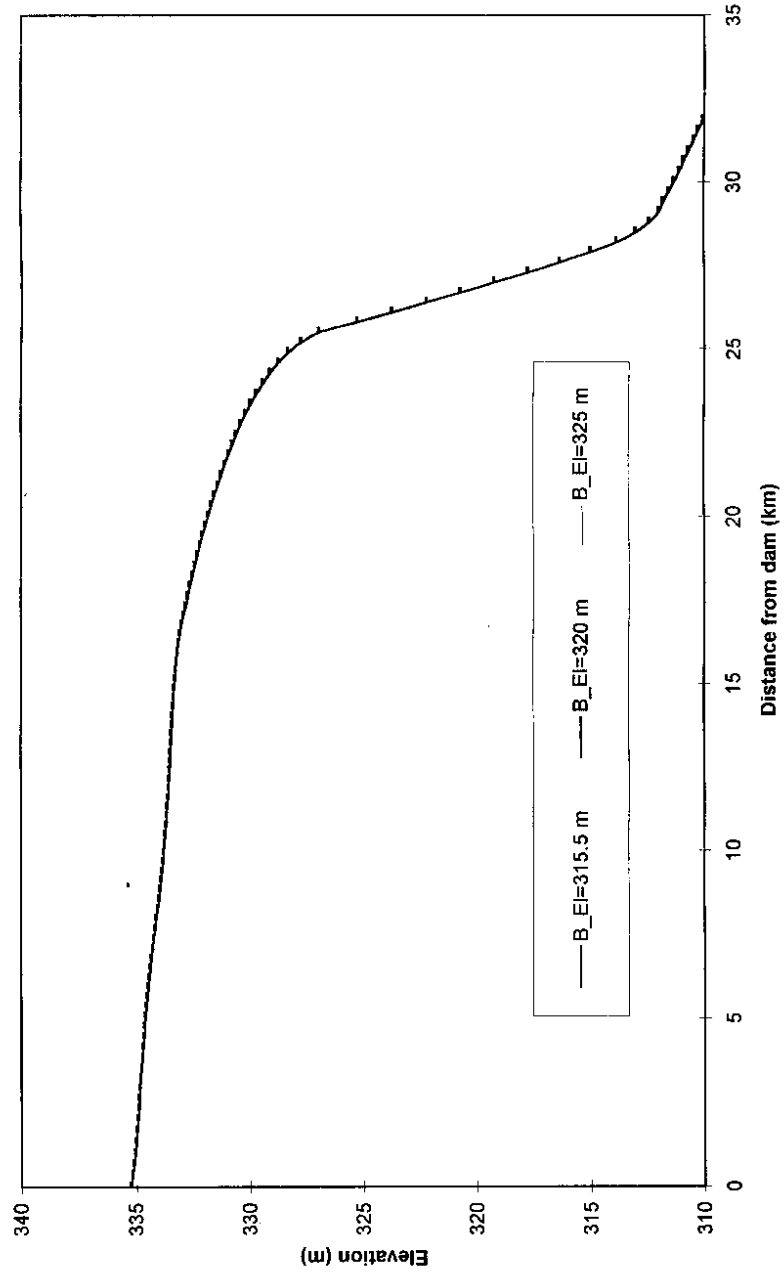


Fig. 8f. Sensitivity of side slope (z) to maximum elevation.

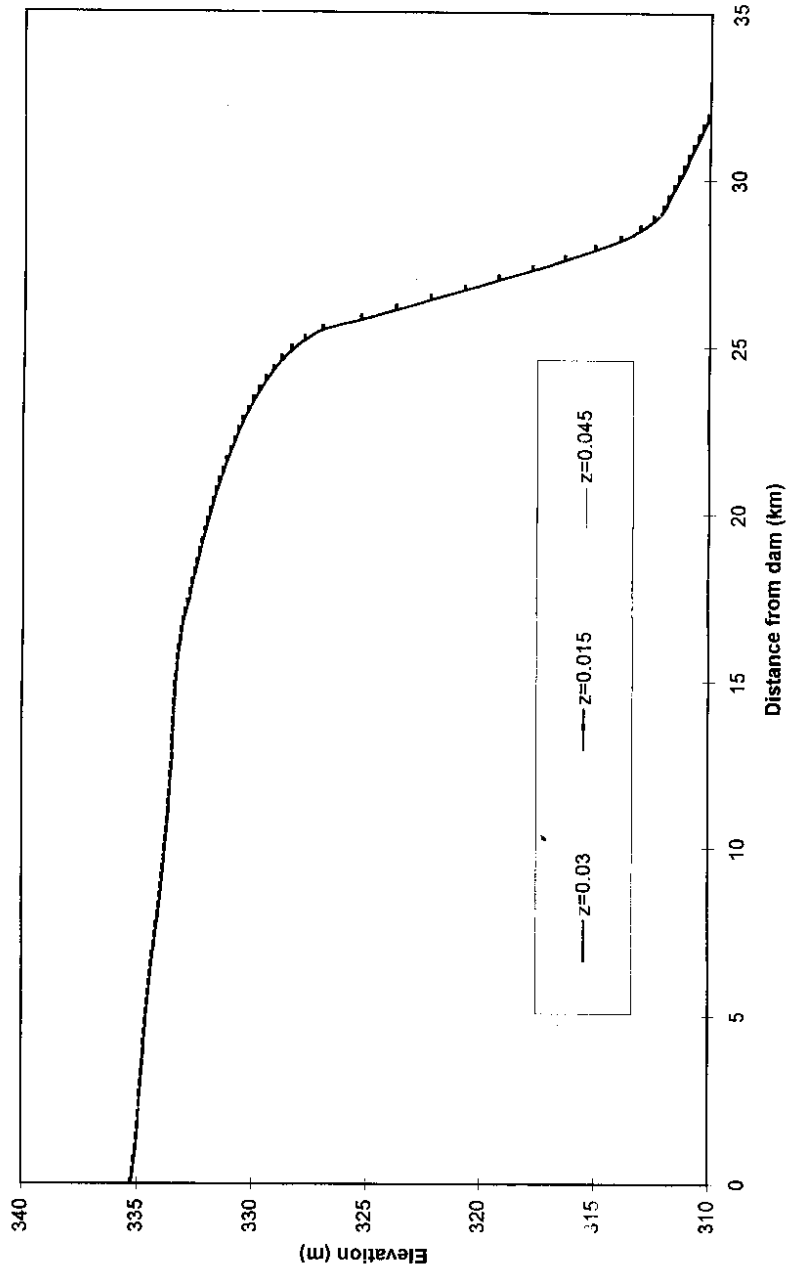


Fig. 8g. Sensitivity of inflow discharge to maximum elevation.

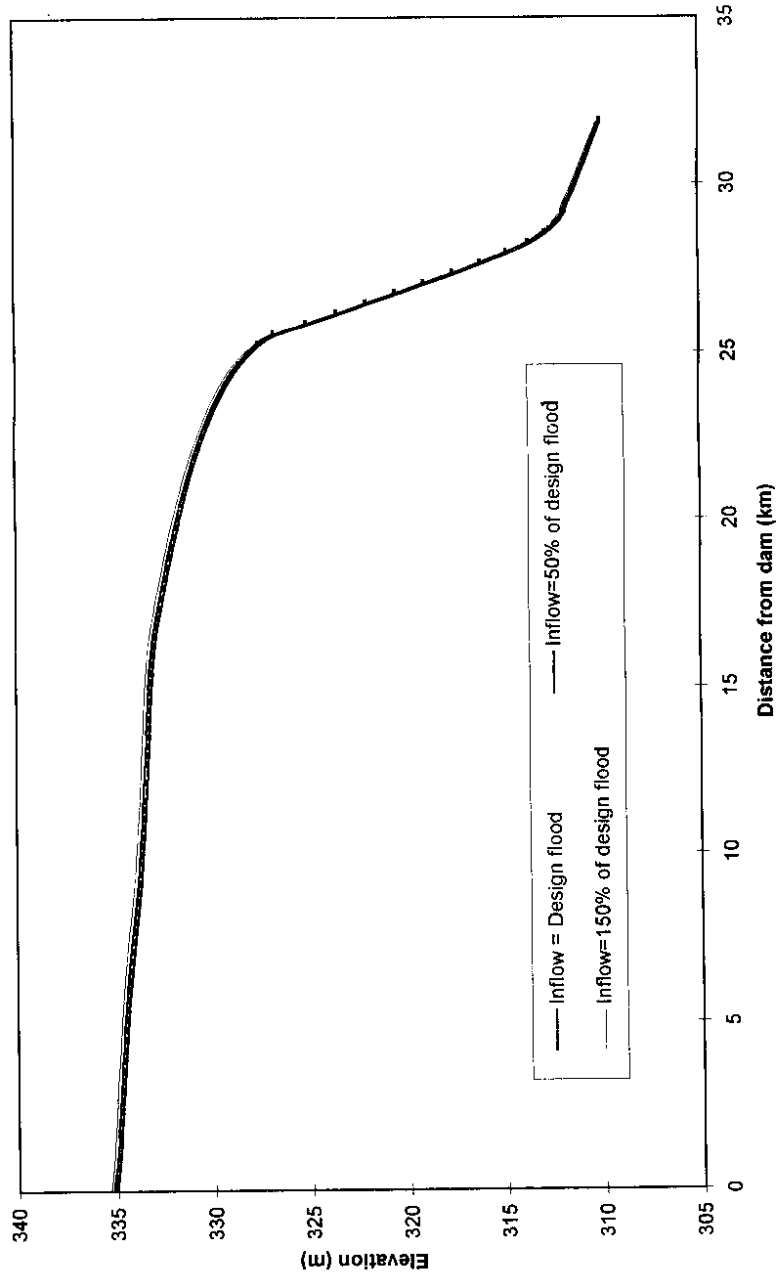


Fig. 9a. Sensitivity of Manning's roughness n to maximum discharge.

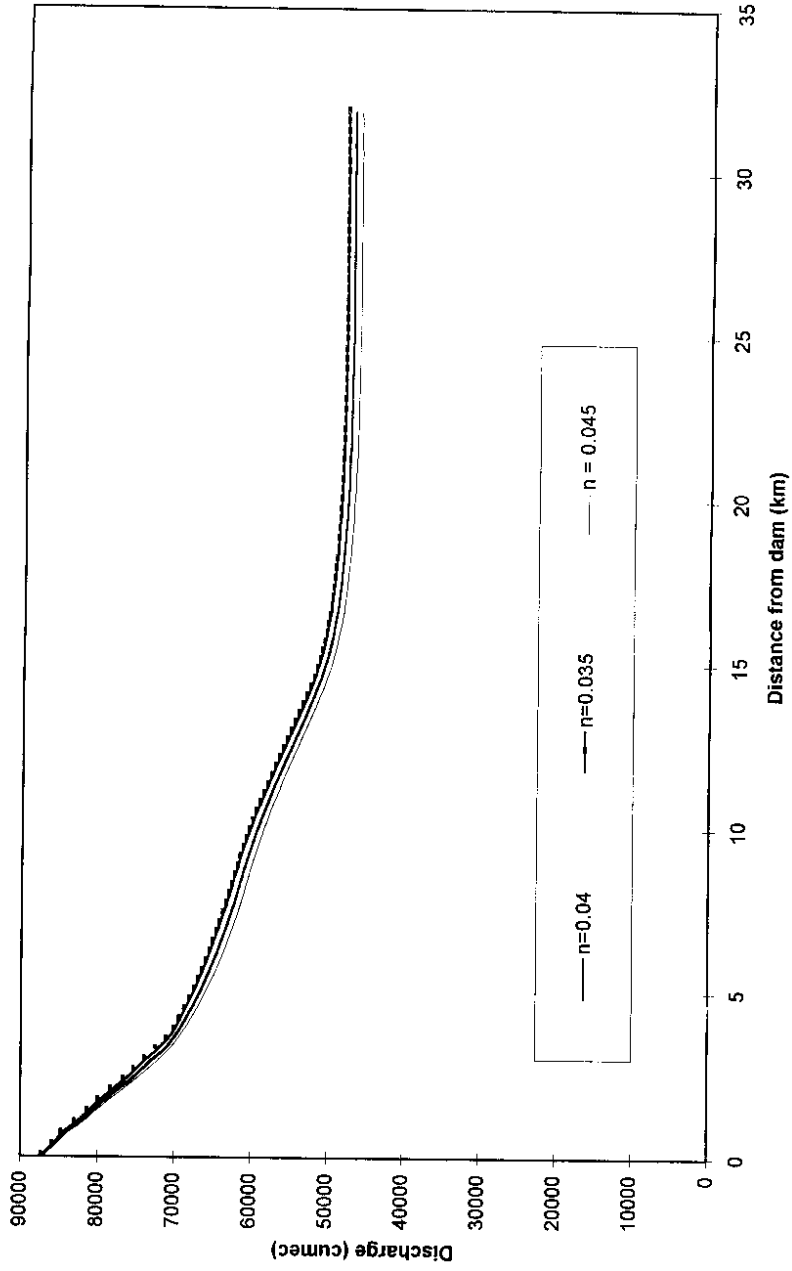


Fig. 9b. Sensitivity of expansion coefficient (Exp) to maximum discharge.

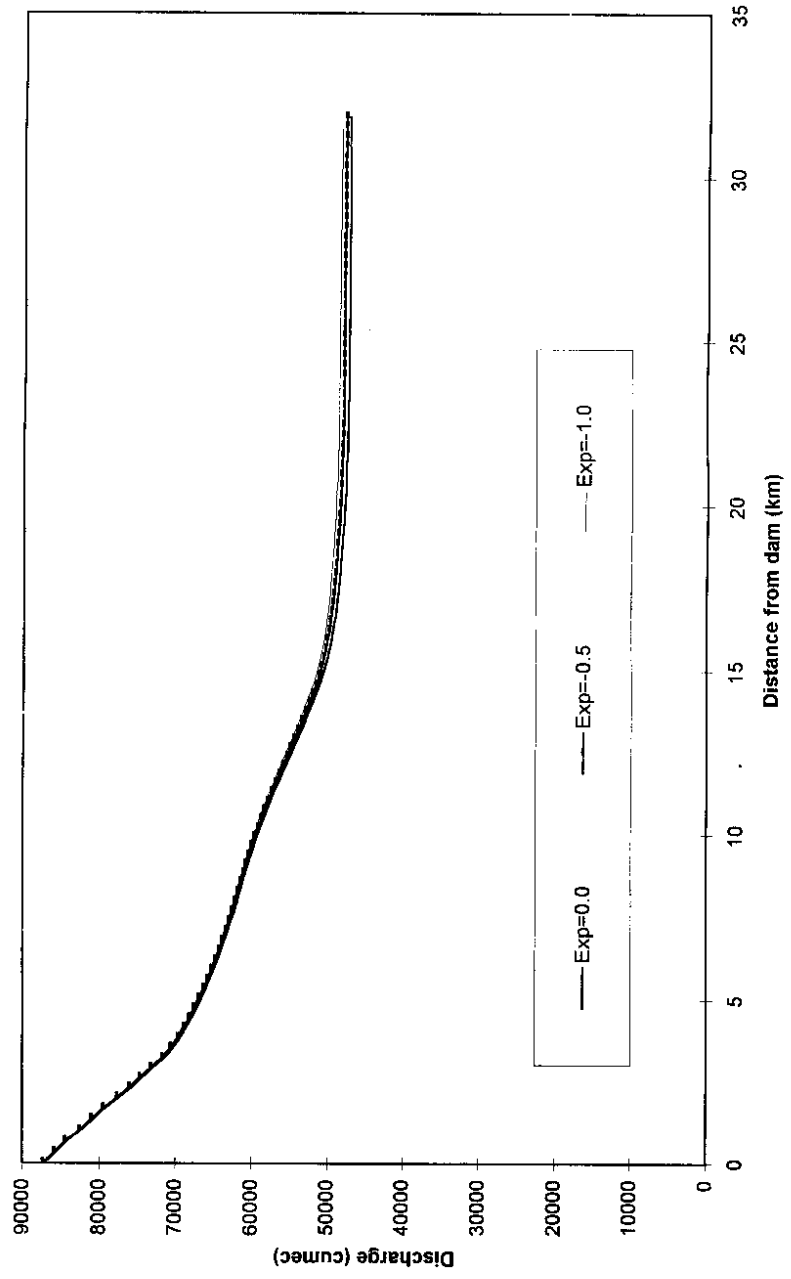


Fig. 9c. Sensitivity of time of failure (t_f) to maximum discharge.

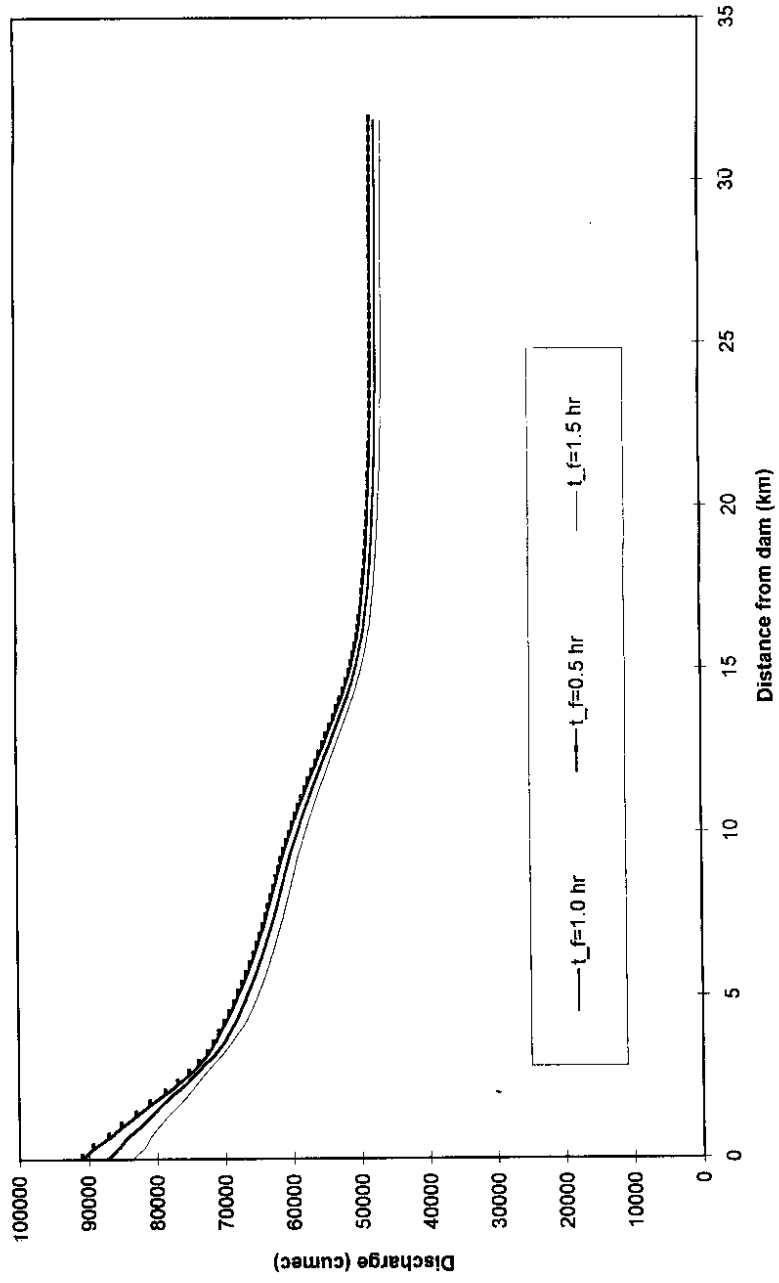


Fig. 9d. Sensitivity of breach width (B_W) to maximum discharge.

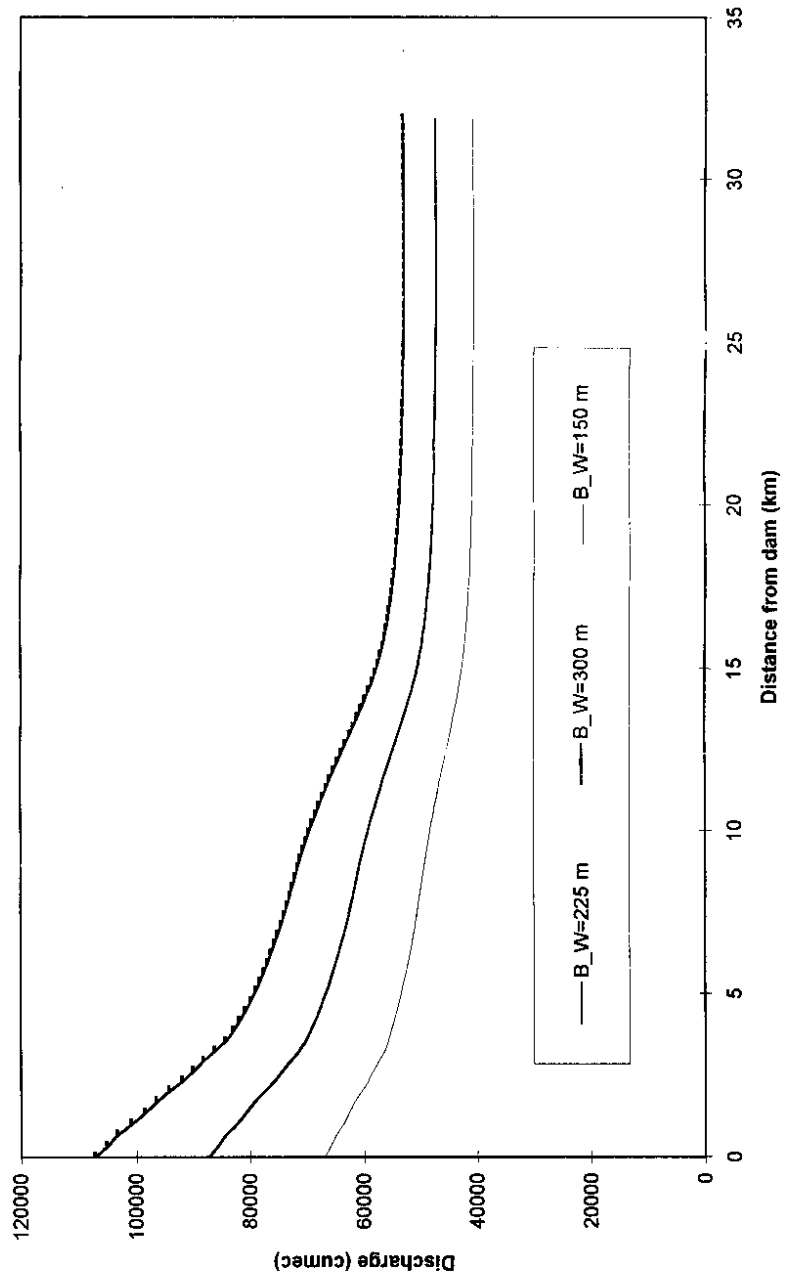


Fig. 9e. Sensitivity of breach elevation (B_EI) to maximum discharge.

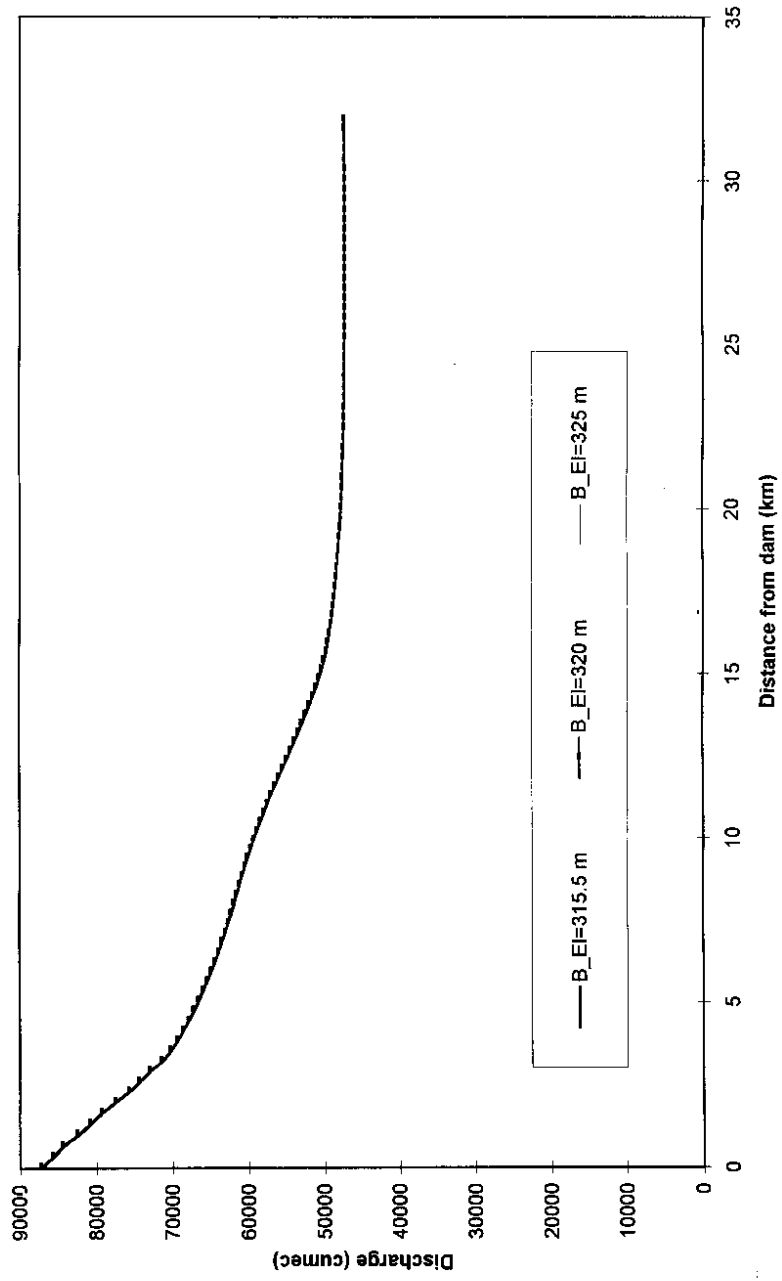


Fig. 9f. Sensitivity of side slope (z) to maximum discharge.

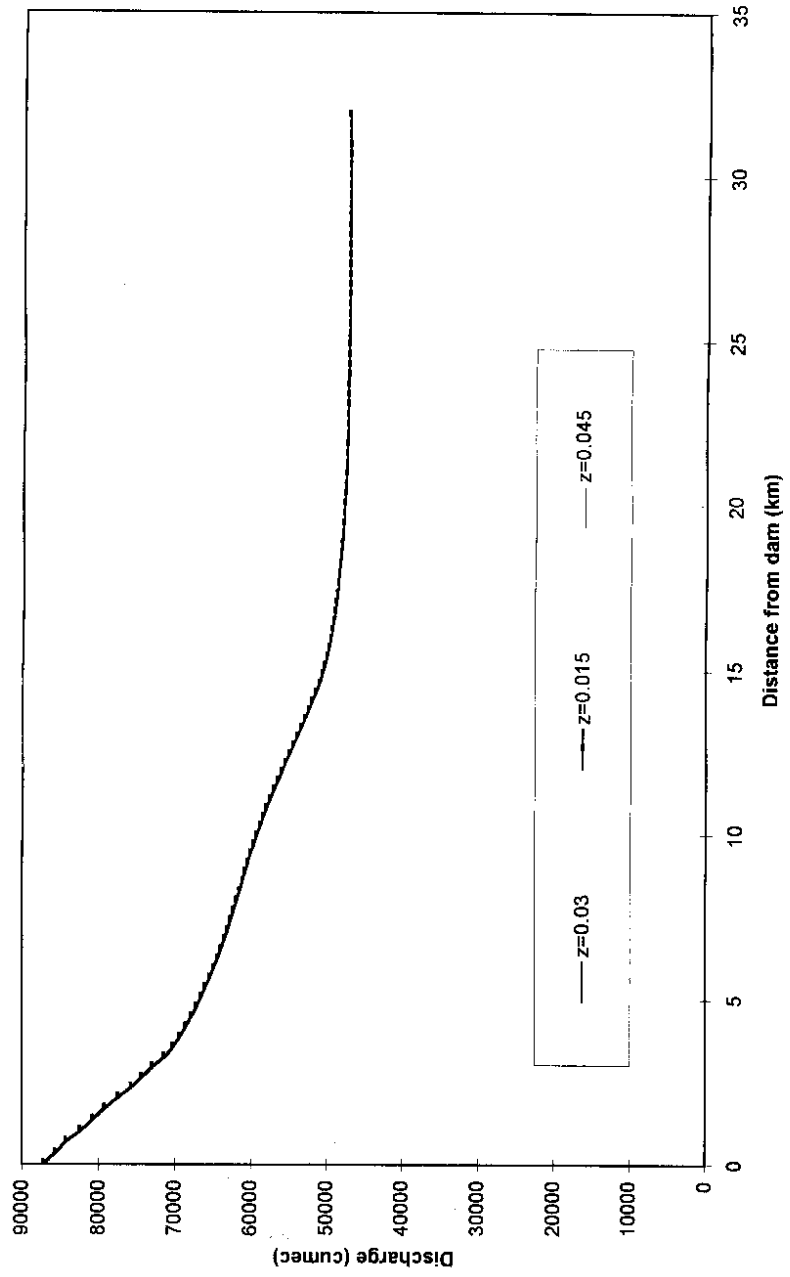
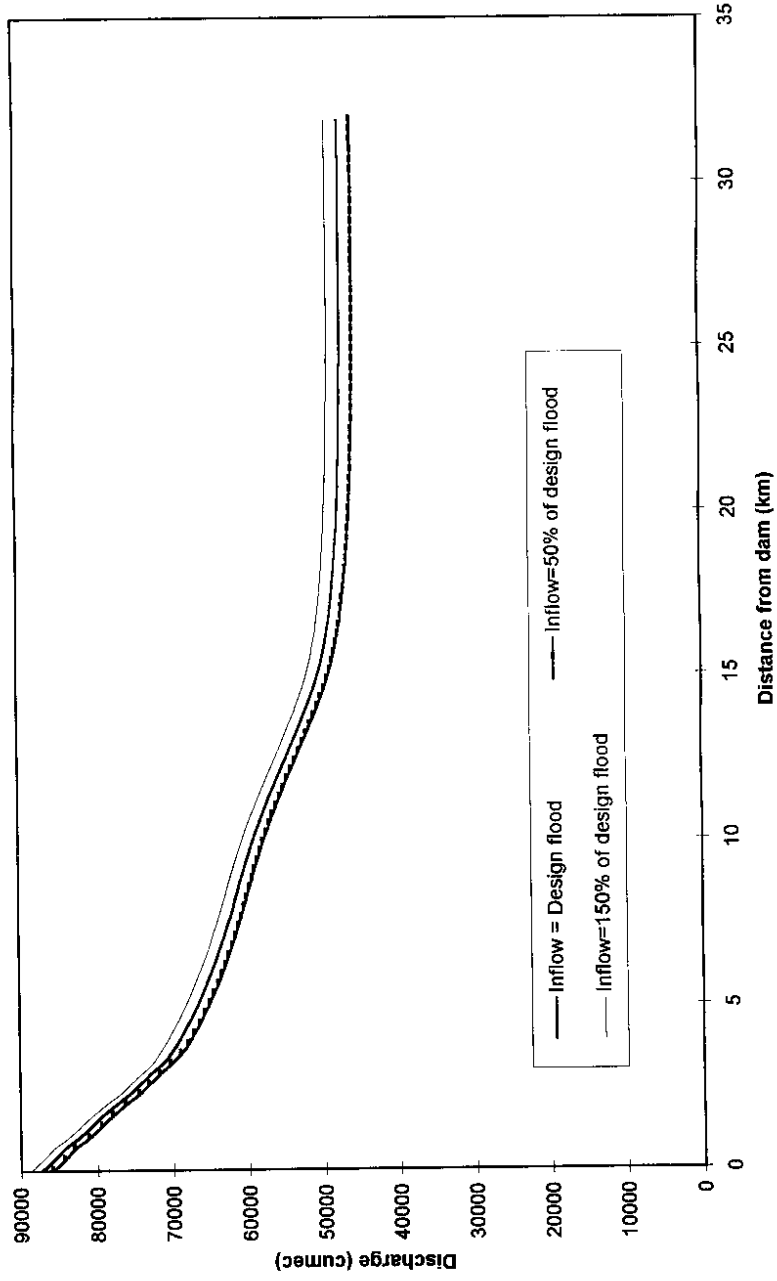


Fig. 9g. Sensitivity of inflow discharge to maximum discharge.



SUMMARY

The present case study of Barna dam break analysis was carried out with a view to estimate the dam break flood hydrograph at the dam site and study its propagation in the downstream portion of the river reach of 32 km where it joins River Narmada. At about 22 km from the dam site, there is Bareli township and the present study would help provide a possible flood scenario in the eventuality of dam failure. The estimated dam break flood magnitude is of the order of 87000 cumec discharging at an elevation of 335.23 m at the dam site and at Bareli, the estimated discharge magnitude is of the order of 47500 cumec with water elevation of 331 m. These results are subjected to the assumed values of dam breach parameters and, therefore, have led to carrying out a sensitivity analysis of those DAMBRK model inputs subject to modeler's judgment.

The considered DAMBRK inputs for sensitivity analysis are: a) Manning's roughness. b) Expansion/contraction coefficients. c) Time of failure. d) Breach width. e) Breach elevation. f) Side slope of the breach section. g) Inflow hydrograph. The effect of these inputs is summarized here in what follows:

- The effect of roughness was less pronounced at higher discharges than at lower discharges and the downstream location of concern was more affected by the Manning's roughness than the dam break flood hydrograph at the dam site. Also, the effect was more pronounced in the mild river reach (before 17 km) than in the steep river reach (after 17 km).
- The variation in the magnitude of expansion coefficient in the prescribed range did not affect elevations except in the most downstream part (after approximately 25 km from dam).
- The effect of time of failure on the maximum water elevation was much less pronounced than the maximum discharge.

┌

- The greater breach width produced greater magnitudes of discharge and corresponding elevation at locations in the river reach and vice versa. The effect almost diminished in the steep river reach (after 17 km).
- The effect of breach elevation on both maximum water elevation and discharge was insignificant for the cases examined.
- The effect of side slope variation from 0.015 to 0.045 on both the maximum water elevation and discharge was insignificant.
- The inflow variation from 50% of design flood to 150% of design flood affected significantly both the maximum discharge and water surface elevation profiles. The effect on discharge was more pronounced in the river portion having steep slope (after 17 km) and the converse was true in the case of elevation.

REFERENCES

- Costa, J.E. (1985). "Floods from dam failures," *U.S. Geological Survey Open-File Rep. 85-560*, Denver, Colo
- Ferrick, M.G.(1985), 'Analysis of river wave types,' *Water Resources Research*, Vol. 21(2), pp. 209-220.
- Fread, D.L. (1980). "DAMBRK - The NWS dam break flood forecasting model." *National Weather Service, Office of Hydrology*, Silver Spring, Maryland.
- Johnson, F.A., and Illes, P. (1976). "A classification on dam failures". *Int. Water Power Dam Construct.*, Dec., pp. 43-45.
- Land, L.F. (1980a). Evaluation of selected dam-break flood wave models by using field Data. *Geol. Surv. Water-Resour. Invest. (U.S.)*, 80-44, 1-54.
- Land, L.F. (1980b). Mathematical simulations of the Toccoa Falls, Georgia, dam-break flood. *Water Resour. Bull.* 16, 1041-1048.
- MacDonald, T.C., and Langridge-Monopolis, J. (1984). "Breaching characteristics of dam failures", *J. Hydr. Engrg.*, ASCE, 110(5), 567-586.
- Mishra, S.K. (1995). "Effect of downstream boundary conditions on the propagation characteristics of dam break flood," *NIH report, BR, NIH*, Roorkee (India).
- Mishra, S.K. and Seth, S.M. (1996). "Use of hysteresis for defining the nature of flood wave propagation in natural channels," *Hydrological Sciences Journal-des Sciences Hydrologiques*, 41(2), April.
- Mishra, S.K., M.K. Jain, and S.M. Seth(1997),"Characterization of flood waves by rating curves,' *J. Nordic Hydrology*, Vol. 28(1).
- Mishra S.K. and Singh, V.P.(1998a)."Hysteresis-based flood wave analysis,' *J. Hydrologic Engineering*, ASCE. (Accepted)
- Mishra S.K. and Singh, V.P.(1998b)."On Seddon speed formula,' *J. Hydrological Sciences*, IAHS. (Submitted)
- Petrascheck, A.W., and Sydler, P.A. (1984). "Routing of dam break floods," *Int. Water Power Dam Construct.* 36, 29-32.

DIRECTOR : DR. S.M. SETH
DIVISIONAL HEAD : SH. R.D. SINGH
SCIENTISTS : SH. S.K. MISHRA
SH. R.D. SINGH